ORIGINAL PAPER

Wojciech Bartkowiak · Paweł Lipkowski

Hydrogen-bond effects on the electronic absorption spectrum and evaluation of nonlinear optical properties of an aminobenzodifuranone derivative that exhibits the largest positive solvatochromism

Abstract In this work, for the first time, a theoretical approach to describing the influence of hydrogen-bond formation on the electronic absorption spectrum and nonlinear optical properties of an aminobenzodifuranone derivative (ABF) that exhibits the largest positive solvatochromic shift compared to other known chromophores is given. The solvent effect was included via the supermolecule (SM) method. The calculations were performed for a strong low-lying ($\pi \to \pi^*$) transition based on the configuration interaction singles (CIS) and time-dependent DFT (TDDFT) methods. The first-order hyperpolarizabilities (β) were computed using the finite-field (FF) technique combined with the Hartree–Fock (HF) theory. Reasonable agreement between theory and experiment was obtained for the solvatochromic shifts of the ABF molecule. Moreover, it was found that H-bond formation strongly influences the NLO response of the systems investigated.

Keywords Solvent effect · Hydrogen bond · Supermolecule · Aminobenzodifuranone · Hyperpolarizability

Introduction

Solvatochromism is connected with the change in position and/or intensity of an electronic absorption band accompanying a change in the polarity of solvent [1, 2]. These changes can be explained based on the theory of intermolecular solute/solvent interactions in the ground (g) and the Franck–Condon excited state (e). In general,

W. Bartkowiak (✉) · P. Lipkowski
Institute of Physical and Theoretical Chemistry,
Wrocław University of Technology,
Wybrzeże Wyspiańskiego 27,
50-370 Wrocław, Poland
E-mail: bartkowiak@kchk.ch.pwr.wroc.pl
E-mail: lipkowsk@mml.ch.pwr.wroc.pl

the solvatochromic shift of the maximum of an absorption band ($\Delta \omega$) is described by the following relation [3]:

$$\Delta\omega = \Delta\omega_E + \Delta\omega_D + \Delta\omega_H \qquad (1)$$

where $\Delta \omega_E$ is the pure electrostatic contribution, $\Delta \omega_D$ the dispersion contribution, and $\Delta \omega_H$ is the connected with the short-range specific interaction between the solvent and solute, e.g. hydrogen bonding.

The largest solvatochromic shifts are observed in the case of donor-acceptor π-conjugated chromophores. The electronic absorption spectra for this type of molecule are characterized by a strong low-lying ($\pi \to \pi^*$) transition assigned to an intramolecular charge-transfer (CT) transition [1, 2, 4–7]. Hence, a large change in the permanent dipole moment during excitation is observed in this case. Because of the difference in the solute/solvent electrostatic interaction energy between the ground and the CT excited states, strong solvatochromic shifts are observed on going from the gas phase to polar solvents. The basic fundamental contributions toward a modern understanding of the solute/solvent electrostatic interactions ($\Delta \omega_E$) on the electronic absorption has been developed by many researchers. Most of the proposed approaches are based on classical Onsager reaction field theory and have been analyzed in a number at monographs and reviews [1, 2, 4–9]. In general, all of these theories, in which a solvent is usually treated as an isotropic dielectric medium characterized by its relative electric permittivity (ϵ_r) and refractive index (n), predict a linear dependence of the solvatochromic shift on the dipole moment difference between the ground and the CT excited states ($\Delta \mu_{gCT}$). For example, Amos and Burrows, based on perturbation theory combined with the reaction field method, derived the following equation describing solvent effects on the transition energy from the ground state to the CT excited state [6]:

$$\hbar\Delta\omega_{CTg} = A\Delta\mu_{CTg}(\mu_{CT} - \mu_g) + B\Delta\mu_{CTg}\mu_g \qquad (2)$$

$$A = \frac{1}{a^3}\frac{n^2-1}{2n^2+1}, \qquad B = \frac{2}{a^3}\frac{\varepsilon_r-1}{2\varepsilon_r+1} - \frac{n^2-1}{2n^2+1}$$

where $\hbar\Delta\omega_{gCT} = \hbar\Delta\omega_{gCT}^{gas} - \hbar\Delta\omega_{gCT}^{sol}$ is the change in transition energy, μ_g the ground state solute dipole moment and μ_{CT} is the excited state dipole moment. The parameter a stands for the radius of a cavity (assumed spherical) occupied by the solute molecule. Based on Eq.2 it is possible to explain easily the direction of the shifts of the absorption bands as the solvent polarity increases (negative and positive solvatochromism) [1, 2, 6, 7]. In the case of positive solvatochromism (i.e. red shift with increasing solvent polarity), the more polar CT excited ($\mu_g < \mu_{CT}$) state is stabilized more than the molecule in the ground state. Hence, the excitation energy is significantly decreased. In the case of negative solvatochromism (blue shift), the ground state is stabilized more by polar solvents as compared to the excited state ($\mu_g > \mu_{CT}$). This leads to an increase of the solute excitation energy with increasing solvent polarity.

The dispersion energy is present in all solvents (polar and nonpolar). In contrast to extensive investigations of the electrostatic solute/solvent interactions ($\Delta\omega_E$) influencing the solvatochromic shifts, the dispersion effect ($\Delta\omega_D$) on the excitation energy of molecules in condensed phases is more complicated for theoretical descriptions [1, 3, 10]. However, it is well established that the dispersion effect always leads to a red shift (positive solvatochromism) of the solvent-induced electronic spectra [1–4, 7, 10]. This is connected with the fact that the excited state exhibits a larger linear polarizability in comparison with the ground state. Hence, the dispersion interaction energy between the excited solute and the environment is substantially larger than in the case of the dispersion interactions for the solute in the ground state. It should be noticed that, in the case of intramolecular CT transitions, the dispersion effect ($\Delta\omega_D$) on the position of the electronic absorption band in polar solvents is less important in comparison with the electrostatic contribution ($\Delta\omega_E$) [1, 2].

Intermolecular hydrogen bond (H-bond) formation has a different effect on the energies of various excited states [1, 3]. It is well established that specific H-bond interactions strongly influence the $n \rightarrow \pi^*$ transition of carbonyl compounds [1–4, 10–12]. In this case, the H-bonding interactions ($\Delta\omega_H$) stabilize the ground state more than the less dipolar-excited state. Hence, solvent induced blue shifts (negative solvatochromism) are observed in H-bond donating solvents. On the other hand, for example, the presence of H-bonds also strongly influences the intensity of the CT absorption ($\pi \rightarrow \pi^*$) band for p-nitroaniline (PNA) [13].

There are also many known examples of theoretical and experimental investigations of the hydrogen bond effects on the nonlinear optical (NLO) response of molecular systems [14–21]. Recently, Keinan et al. [15] have shown that the H-bond formation between optically active chromophores enhances the values of

first-order hyperpolarizability (β) in comparison with isolated monomers. This observation can be used for a rational design of electrooptic materials. A substantial solvent effect on β is also observed for small organic and inorganic molecules [19, 20]. The sign of β for solvated water and urea changes as compared to the gas phase. This is connected with the fact that these molecules may form H-bonds with solvent molecules. Another important example is PNA. The PNA molecule can form H-bonds between the NH_2 group and H-bond donor groups of the solvent. Huyskens et al. [21] have shown that the formation of specific H-bond solute/solvent interactions always increases the value of β.

Recently, it has been shown by Gorman et al. [22] that an aminobenzodifuranone derivative (3-(4-amino-3-methyl-phenyl)-7-phenyl-3,7-dihydro-benzo[1,2-b;4,5-b'] difuran-2,6-dione; ABF) exhibits the largest positive solvatochromic shift compared to other known chromophores (Fig.1; molecule **I**). Experimentally, the maximum long-wavelength absorption ($\pi \rightarrow \pi^*$) band of ABF shifts from $\sim v = 20076$ cm^{-1} in nanofluoro-it tert-butyl alcohol (NFTB) to $\sim v = 14201$ cm^{-1} in hexamethylphosphortriamide (HMPA). It has been suggested that the solvatochromic behavior of ABF is associated with the H-bond donating and accepting properties of its NH_2 group. Schematic structures of the molecule **I** hydrogen bonded with NFTB (complex **II**) and HMPA (complex **III**) as suggested by Gorman et al. [22] are shown in Fig.1. Recently, the solvatochromic behavior of ABF has been investigated based on discrete simulations based on the quantum-mechanical Langevine dipoles/Monte Carlo (QM/LD/MC) technique as well as continuum models [23]. However, the results of these investigations have not confirmed the experimentally observed large solvatochromic shift of the low-lying absorption band of ABF. Hence, a theoretical description of the solvatochromism of ABF is still a challenge
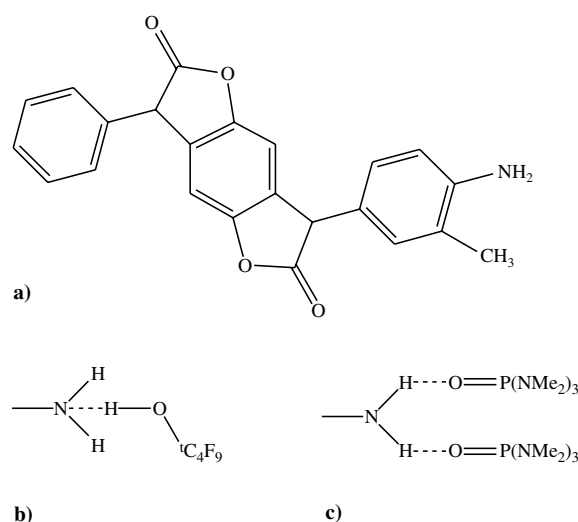

Fig. 1 A schematic structures of the studied systems: **a** I—ABF; **b** II—complex ABF with NFTB; **c** III—complex ABF with HMPA

for quantum chemical methods. This example offers a unique opportunity for testing quantum chemical models routinely used the molecular structure investigations.

The aim of this work is a qualitative and quantitative analysis of the significant influence of solvents on the electronic absorption as well as first-order hyperpolarizability (β) of ABF. In particular, the mechanism of the large positive solvatochromism of ABF was examined by carrying out calculations where the solvent influence was described on the supermolecule method (SM) level.

Methods and calculations

The ground state geometries of the isolated molecule **I** and its molecular complexes **II** and **III** were fully optimized without symmetry restrictions using the density functional method (DFT) with hybrid B3LYP functional [24, 25]. The geometry of the complexes correspond to minima since no imaginary frequencies were detected. The standard 6-31G(d,p) basis set was used at this level of theory. Structural analysis was carried out with the GAUSSIAN 03 set of programs [26]. The optimized geometries were then used as the basis for the spectroscopic and NLO property calculations. Ab initio configuration interaction singles (CIS) [27] and time-dependent DFT (TDDFT) [28–30] methods with a 6-31G basis set were used to calculate the vertical transition energies and other spectroscopic parameters (oscillator strengths f as well as the change in dipole moments μ). In this work, the shifts in calculated electronic excitation energies were not corrected for basis set superposition errors (BSSEs).

The tensor components of the static first-order hyperpolarizability (β_{ijk}) were evaluated at the HF/6-31G level using the finite-field method [31, 32]. The finite-field approach (FF) employing energy expansion was used to calculate static β. The total energy E under the influence of the static electric field F can be expanded as a Taylor series:

$$E(\bar{F}) = E(0) - \mu_i F_i - (1/2!)\alpha_{ij}F_iF_j - (1/3!)\beta_{ijk}F_iF_jF_k - (1/4!)\gamma_{ijkl}F_iF_jF_kF_l - \cdots$$

(3)

where $E(0)$ is the energy of molecule without external electric field ($F=0$), μ_i, α_{ij}, β_{ijk}, and γ_{ijkl} are the permanent dipole moment, the dipole polarizability, the first-order and second-order hyperpolarizability, respectively. From the theoretical point of view, according to Eq.3, the components of the β_{ijk} tensor are obtained as the third derivative of the energy with respect to the applied electric field. It should be noted that the default setting for the FF/HF method in the GAUSSIAN 03 package [26] was chosen for the calculations of β.

The calculated components of the β_{ijk} tensor were transformed to the vector quantity (experimentally available quantity for polar molecules) defined as [33]:

$$\beta_\mu = \sum_i \frac{\beta_i \mu_i}{|\mu|}, \quad i \in (x,y,z)$$

with

$$\beta_i = \frac{3}{5}\sum_i \beta_{ijj}, \quad j \in (x,y,z)$$

where μ is the ground state molecular dipole moment.

The level of the quantum chemical methods used in this work is connected with a compromise between quality and computational cost. Because of the size of the molecules studied, the unpolarized 6-31G basis set was used for calculations of the excitation energies and hyperpolarizabilities. The 6-31G basis set is very often used in theoretical investigations of the NLO properties of large organic molecules [34].

Results and discussion

The general strategy of calculations reported in this paper was to check the applicability of the supermolecule method (SM) to predict the largest red shift of the longest-wavelength absorption ($\pi \to \pi^*$) band of **I** in comparison with other known solvatochromic compounds. As previously noted, Gorman et al. [22] in their experimental work have proposed that the origin of this large solvatochromic shift $\left(\Delta\tilde{v} = 5876\,cm^{-1}\right)$ is connected with the H-bond donating and accepting properties of the NH_2 group [22]. The NH_2 group can act both as a proton acceptor (complex **II**) and a proton donor (complex **III**) in hydrogen bonding. Moreover, these authors have indicated that the H-bond accepting ability of NH_2 is enhanced by a larger pyramidalization of this group [22]. This is due to strong steric effects that result from the short distance between the NH_2 and CH_3 groups (see Fig.1). Analysis of the experimental data shows that the solvatochromic shift of the electronic transition of **I** (relative to the energy obtained in non-polar cyclohexane) is larger for HMPA compared to NFTB (see Table 1). This observation indicates that the effect of complexation with HMPA on the electronic structure of **I** is substantially larger than in the case of NFTB. This is also seen in the values of the calculated ground state dipole moments collected in Table 1. This conclusion is supported by a picture of the changes in electronic density (for the ground state) during the formation of H-bonds between ABF and NFTB as well as ABF and HMPA. The isodensity maps plotted in Fig.2 were obtained as a difference between the total electronic density (obtained at the DFT/B3LYP/6-31G(d,p) level) of H-bond complexes and the appropriate density distributions of the isolated monomers [35, 36]. Visualization of the changes in the electronic density distributions of monomers caused by the intermolecular interactions supplements the experimental observation that the electronic structure of **I** is more modified by H-bond

Table 1 The predicted vertical $\pi \rightarrow \pi^*$ excitation energies ($\tilde{v}_{max}$, cm^{-1}), dipole moments (μ, D) in the ground (g) and excited (e) state, and oscillator strengths (f) for ABF (**I**) as well as for ABF-NFTB (**II**) and ABF-HMPA (**III**) complexes at the different levels of theory

Systems	TDDFT			CIS				Exp. [22]
	μ_g	f	$\tilde{v}_{max}$	μ_g	μ_e	f	$\tilde{v}_{max}$	$\tilde{v}_{max}$
I	5.21	0.9305	17283	3.88	7.37	2.2933	24997	18551[a]
II	4.03	1.0283	19043	4.61	3.96	2.3802	26927	20076[b]
III	18.22	1.1311	15488	16.78	21.39	2.2753	20690	14201[c]

[a] In cyclohexane
[b] In nanofluoro-it tert-butanol alcohol (NFTB)
[c] In hexamethylphosphorictriamide (HMPA)

formation with two molecules of HMPA (complex **III**) than in the case of the ABF-NFTB complex (**II**).

To investigate the solvent effect on the absorption spectrum of **I–III**, CIS and TDDFT calculations with the 6-31G basis set were performed. The results of calculations of the vertical transition energy of the first low-lying singlet excited state for the systems investigated are shown in Table 1. As we can see, values of the computed excitation energies as well as spectral shifts depend on the method used in the calculations. A comparison with experimental transitions energies shows that their absolute values are substantially overestimated by the CIS method. These discrepancies are expected because it is well known that the absolute values of the calculated excitation energies using the CIS method overestimate the energy differences between ground and excited states [27, 37, 38]. On the other hand, the TDDFT method has recently been shown to yield relatively accurate excita-

tion energies even for large molecules [17, 28, 29, 39, 40]. Results of our calculations support this observation. It was found that the $\pi \rightarrow \pi^*$ excitation energies predicted by the TDDFT method are closer to the experimental results than the CIS-calculated values. It should be noted that the solvatochromic shift ($\Delta\tilde{v} = 6237$ cm^{-1}) computed at the CIS level on going from NFTB to HMPA as solvent agrees much better with the experimental value ($\Delta\tilde{v} = 5876$ cm^{-1}) than the value obtained from TDDFT ($\Delta\tilde{v} = 3555$ cm^{-1}). However, in the case of the SM approach only short-range solute/solvent interactions (associated with the first solvation shell) are included. For a better description of the solvent effect on the excitation energy, the long-range dielectric (bulk) effect should also be considered [19, 20]. This important limitation should lead to an underestimated calculated value of the solvatochromic shift within the SM approach. Therefore, one can conclude that the TDDFT

Fig. 2 The interaction difference density maps of the studied systems: a **II** complex ABF with NFTB; b **III**—complex ABF with HMPA. *Red color* designates an increase of the electron density caused by the intermolecular interactions, whereas *blue* indicates a coresponding decrease of the electron density. The isodensity contours were plotted for ± 0.01 electron/bohr^3 (DFT/B3LYP/6-31G(d,p))
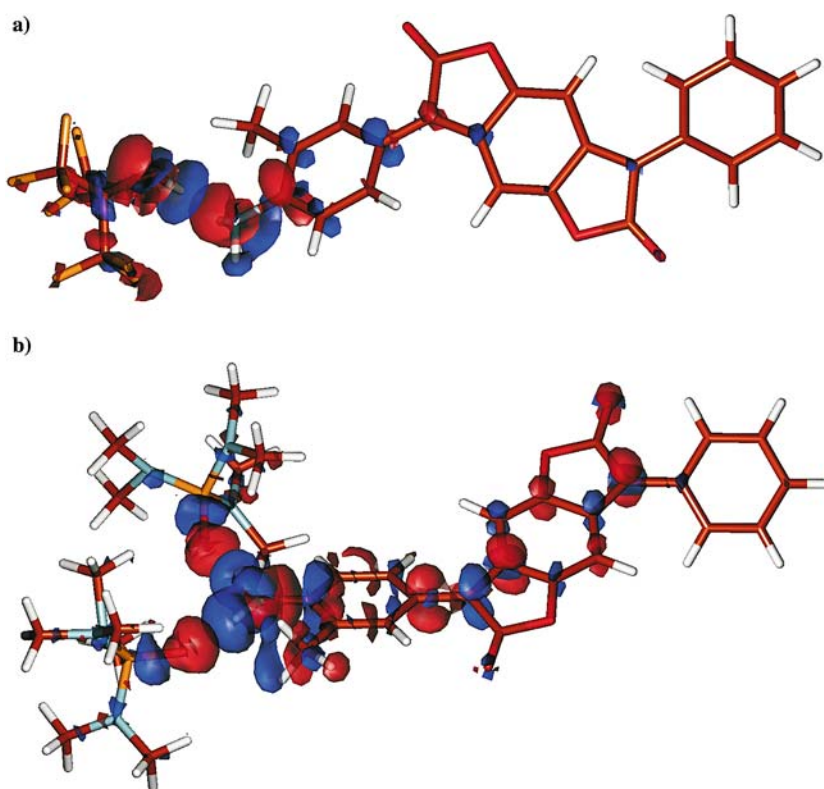
method provides more reliable solvatochromic shifts in our case. However, it should be noted that the quantum chemical calculations based on the TDDFT method as well as the CIS method combined with the SM technique successfully confirm most of the experimental observations.

Figure 3 shows the frontier orbitals of **I–III** at the DFT level. From the CI coefficient of the lowest excited state of the investigated molecules, it was found that the major electronic transition is HOMO $\rightarrow$ LUMO, and the lowest ($\pi \rightarrow \pi^*$) excited state is characterized by this transition. The contributions from other electronic configurations are very small and can be approximately neglected. In the cases of isolated molecule **I** and H-bond complex **III** the qualitative characteristics of the HOMOs and LUMOs indicate that the central cyclic π-system acts as electron-withdrawing group and NH_2 group acts as electron-donating group. From these considerations, the lowest excited states are characterized by a strong intramolecular CT state. However, the CT character of the lowest excited state is enhanced by the presence of a H-bond accepting solvent (HMPA) compared to the isolated molecule **I**, while the H-bond formation between ABF and NFTB (complex **II**) leads to only small changes in electron density upon excitation from HOMO to LUMO. This simple picture based on frontier molecular orbitals is supported by the calculated values of the permanent dipole moment in the ground and excited states (Table 1). The largest change in the calculated permanent dipole ($\Delta \mu \approx 5D$) upon excitation is observed for **III**.

In Table 2, the computed first-order hyperpolarizabilities (β_μ) of the isolated molecule **I**, dimer (**II**), and trimer (**III**) are given. As we can see, the influence of the H-bond effect on β_μ is very substantial. The results of the FF/HF/6-31G calculations of β_μ indicate that the following sequence holds for molecules investigated here: β_μ (**III**) > β_μ (**I**) > β_μ (**II**). This means that the H-bond formation substantially enhances the NLO optical response in the case of complex **III**. The computed static value of β_μ for **III** is three orders of magnitude larger than that of PNA taken as reference. Unfortunately, there is no experimental value available for β_μ for ABF in solution. It should be noted that the FF method is limited to static fields only. In the case of the second-harmonic generation (SHG) dispersion effect, this is significant and always leads to an enhancement of the NLO response of molecular systems [41]. Moreover, the electron-correlation contribution is not included at the FF/HF level. However, in our opinion, the above results can be employed further in the effective molecular design of efficient NLO chromophores.

In conclusion, the specific H-bond influence on the experimentally observed large solvatochromic shift of the low-lying absorption band of ABF was confirmed theoretically for the first time. Spectroscopic parameters

Table 2 Calculated values of the static first-order hyperpolarizabilities (β_μ) for ABF (**I**) as well as for ABF-NFTB (**II**) and ABF-HMPA (**III**) complexes investigated in the present study

Systems	β_μ (10^{-30} esu)
I	44.6
II	−11.8
III	154.3

Fig. 3 Frontier molecular orbitals of the studied systems: **I**—ABF; **II**—complex ABF with NFTB; **III**—complex ABF with HMPA
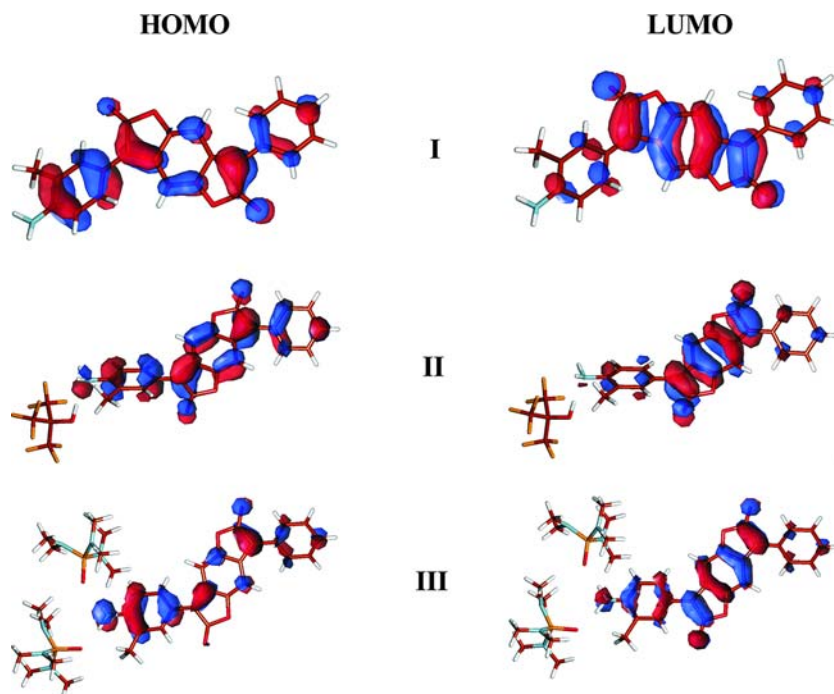
were calculated using the TDDFT and CIS methods combined with the supermolecule (SM) approach. Reasonable agreement between theory and experiment was obtained for the solvatochromic shifts of ABF. Moreover, it was found that H-bond formation strongly influences the NLO response of the systems investigated.

References

1. Reichardt C (1988) Solvents and solvent effects in organic chemistry. VCH, Weinheim
2. Reichardt C (1994) Chem Rev 94:2319–2358
3. Li J, Cramer CJ, Truhlar DG (2000) Int J Quantum Chem 77:264–280
4. Cramer CJ, Truhlar DG (1999) Chem Rev 99:2161–2200
5. Suppan P (1990) J Photochem Photobiol A 50:293–330
6. Amos AT, Burrows BL (1973) In: Advances in quantum chemistry. Academic Press, New York, pp289–313
7. Liptay N (1974) In: Excited states. New York, pp129–229
8. Tomasi J, Persico M (1994) Chem Rev 94:2027–2094
9. Warshel A (1991) Computer modeling of chemical reactions in enzyme and solutions. Wiley, New York
10. Grozema FC, van Duijnen PT (1998) J Phys Chem A 102:7984–7989
11. Gao J (1994) J Am Chem Soc 116:9324–9328
12. Fox T, Rösch N (1992) Chem Phys Lett 191:33–37
13. Kovalenko SA, Schanz R, Farztdinov VM, Henning H, Ernsting NP (2000) Chem Phys Lett 323:312–322
14. Zyss J, Chemla DS (eds) (1987) Nonlinear properties of organic molecules and crystals. Academic Press, Orlando
15. Keinan S, Ratner MA, Marks TJ (2004) Chem Mater 16:1848–1854
16. Maroulis G (2000) J Chem Phys 113:1813–1820
17. Wang C-K, Wang Y-H, Su Y, Luo, Y (2003) J Chem Phys 119:4409–4412
18. Wu K, Snijders JG, Lin C (2002) J Phys Chem B 106:8954–8958
19. Mikkelsen KV, Luo Y, Ågren H, Jorgensen P (1995) J Phys Chem 102:9362–9367
20. Bartkowiak W, Zaleśny R, Kowal M, Leszczynski J (2002) Chem Phys Lett 362:224–228
21. Huyskens FL, Huyskens PL, Persoons AP (1998) J Chem Phys 108:8161–8171
22. Gorman AA, Hutchings MG, Wood PD (1996) J Am Chem Soc 118:8497–8498
23. Bartkowiak W (2000) Synth Met 109:108–111
24. Lee C, Yong W, Parr RG (1988) Phys Rev B 37:785–789
25. Becke AD (1992) J Chem Phys 98:1372–1377
26. Frisch MJ, Trucks GW, Schlegel HB, Scuseria GE, Robb MA, Cheeseman JR, Montgomery JA Jr, Vreven T, Kudin KN, Burant JC, Millam JM, Iyengar SS, Tomasi J, Barone V, Mennucci B, Cossi M, Scalmani G, Rega N, Petersson GA, Nakatsuji H, Hada M, Ehara M, Toyota K, Fukuda R, Hasegawa J, Ishida M, Nakajima T, Honda Y, Kitao O, Nakai H, Klene M, Li X, Knox JE, Hratchian HP, Cross JB, Adamo C, Jaramillo J, Gomperts R, Stratmann RE, Yazyev O, Austin AJ, Cammi R, Pomelli C, Ochterski JW, Ayala PY, Morokuma K, Voth GA, Salvador P, Dannenberg JJ, Zakrzewski VG, Dapprich S, Daniels AD, Strain MC, Farkas O, Malick DK, Rabuck AD, Raghavachari K, Foresman JB, Ortiz JV, Cui Q, Baboul AG, Clifford S, Cioslowski J, Stefanov BB, Liu G, Liashenko A, Piskorz P, Komaromi I, Martin RL, Fox DJ, Keith T, Al-Laham MA, Peng CY, Nanayakkara A, Challacombe M, Gill PMW, Johnson B, Chen W, Wong MW, Gonzalez C, Pople JA (2004) Gaussian 03, Revision C.02. Gaussian Inc, Wallingford CT
27. Foresman JB, Head-Gordon M, Pople JA, Frish MJ (1992) J Phys Chem 96:149–135
28. Bauernschmitt R, Ahlrichs R (1996) Chem Phys Lett 256:454–464
29. Stratmann RE, Scuseria GE, Frisch MJ (1998) J Chem Phys 109:8218–224
30. Casida ME, Jamorski C, Casida RC, Salahub DR (1998) J Chem Phys 108:4439–4449
31. Cohen HD, Roothaan CC (1965) J Chem Phys 55:S43
32. Kurtz HA, Stewart JJP, Dieter KM (1990) J Comput Chem 11:82–87
33. Bishop DM, Norman P (2000) In: Handbook of advanced electronic and photonic materials and devices. Academic Press, San Diego, pp1–240
34. Champagne B, Kirtman B (2000) In: Handbook of advanced electronic and photonic materials and devices. Academic Press, San Diego, pp63–126
35. Gora RW (2001–2003) DENDIF v2.1.1 package, Wroclaw, Poland, Jackson, MS, USA
36. Schaftenaar G, Noordik JH (2000) J Comput-Aided Mol Design 14:123–134
37. Jasien PG, Weber LL (2001) J Mol Struct (Theochem) 572:203–212
38. Abe J, Shirai Y (1996) J Am Chem Soc 118:4705–4706
39. Sałek P, Vahtras O, Helgaker T, Ågren H (2002) J Chem Phys 117:9630–9645
40. Masunov A, Tretiak S (2004) J Phys Chem B 108:899–907
41. Kanis DR, Ratner MA, Marks TJ (1994) Chem Rev 94:195–242